

000 001 002 003 004 005 006 007 008 009 010 011 012 013 014 015 016 017 018 019 020 021 022 023 024 025 026 027 028 029 030 031 032 033 034 035 036 037 038 039 040 041 042 043 044 045 046 047 048 049 050 051 052 053 DOES GENERATIVE RETRIEVAL BREAK THROUGH THE LIMITATIONS OF DENSE RETRIEVAL?

Anonymous authors

Paper under double-blind review

ABSTRACT

Generative retrieval (GR) has emerged as a new paradigm in neural information retrieval, offering an alternative to dense retrieval (DR) by directly generating identifiers of relevant documents. In this paper, we theoretically and empirically investigate how GR fundamentally diverges from DR in both learning objectives and representational capacity. GR performs globally normalized maximum-likelihood optimization and encodes corpus and relevance information directly in the model parameters, whereas DR adopts locally normalized objectives and represents the corpus with external embeddings before computing similarity via a bilinear interaction. Our analysis suggests that, under scaling, GR can overcome the inherent limitations of DR, yielding two major benefits. First, with larger corpora, GR avoids the sharp performance degradation caused by the optimization drift induced by DR’s local normalization. Second, with larger models, GR’s representational capacity scales with parameter size, unconstrained by the global low-rank structure that limits DR. We validate these theoretical insights through controlled experiments on the Natural Questions and MS MARCO datasets, across varying negative sampling strategies, embedding dimensions, and model scales. But despite its theoretical advantages, GR does not universally outperform DR in practice. We outline directions to bridge the gap between GR’s theoretical potential and practical performance, providing guidance for future research in scalable and robust generative retrieval.

1 INTRODUCTION

Advances in deep learning and representation learning (Vaswani et al., 2017; Lee & Toutanova, 2018) have established neural information retrieval (IR) as the dominant paradigm (Mitra et al., 2018; Fan et al., 2022). Within this paradigm, dense retrieval (DR) encodes queries and documents into vectors and measures their similarity through bilinear interactions, enabling efficient vectorized recall and delivering state-of-the-art performance across diverse retrieval tasks (Karpukhin et al., 2020; Khattab & Zaharia, 2020). Recently, driven by generative large language models (LLMs) (Radford et al., 2018; Yang et al., 2025b; Lewis et al., 2020), generative retrieval (GR) has emerged as a new branch of neural IR (Tay et al., 2022; Bevilacqua et al., 2022; Zhuang et al., 2022; Wang et al., 2022; Li et al., 2024; Zeng et al., 2024b). GR directly generates identifiers of relevant documents (docids) for a given query, with corpus knowledge embedded in the model parameters. It typically adopts a sequence-to-sequence architecture trained with cross-entropy loss, while inference relies on constrained decoding to ensure valid docids.

To better understand GR, recent studies have examined its connection to DR. Some research interprets GR as implicitly performing dot-product scoring within an LLM’s parameters and propose a unified framework for similarity computation across both paradigms (Nguyen & Yates, 2023; Wu et al., 2024). Despite this formal unification, the substantial differences in model architecture should not be overlooked: DR is encoder-only, whereas GR employs an autoregressive model with a decoder. This naturally raises the question:

Do GR and DR differ fundamentally in their modeling mechanisms for retrieval?

We address this question along two dimensions: (i) *Learning objective*: DR trains with local normalization over a small candidate set in document space, whereas GR maps the problem to vocabulary space and optimizes a globally normalized likelihood; and (ii) *Representational capacity*:

054 DR encodes queries and documents as low-dimensional embeddings, while GR uses the full model
 055 parameters to memorize the entire corpus.
 056

057 Our **theoretical analysis** elaborates on these aspects and leads to the following conclusions: DR has
 058 intrinsic bottlenecks in both learning and representation that constrain its performance under scaling
 059 of corpus and model size, whereas GR does not. First, local normalization in DR introduces calibration
 060 errors that grow with corpus size, whereas GR’s global normalization avoids such optimization
 061 drift and benefits more from larger corpora. Second, the low-rank constraint imposed by DR’s em-
 062 bedding dimension limits its ability to approximate the (often higher-rank) true query-document
 063 relevance matrix, whereas GR’s parameterization allows higher-rank approximations, making it bet-
 064 ter suited to leverage large-scale models.

065 To validate our theoretical analysis **empirically**, we evaluate standard DR, multi-vector DR
 066 (MVDR) (Khattab & Zaharia, 2020; Formal et al., 2021; Li et al., 2023a) and two GR variants
 067 following the DSI (Tay et al., 2022) framework on the Natural Questions (NQ) (Kwiatkowski et al.,
 068 2019) and MS MARCO (Bajaj et al., 2016) datasets. Under controlled settings, we conduct three
 069 studies: (i) By varying DR’s negative sampling and embedding dimension, we evaluate their effects
 070 on calibration error and ranking metrics; experimental results show optimization limits due to local
 071 normalization and representation limits due to the embedding dimension. (ii) By scaling GR and DR
 072 with matched model sizes and training corpus sizes, we observe larger gains for GR, providing pre-
 073 liminary evidence that GR has the potential to overcome DR’s bottlenecks when scaled. (iii) Using
 074 a larger model with 14B parameters, we conduct zero-shot and test-time scaling experiments for GR
 075 and observe promising performance, further supporting the scaling advantages that GR may obtain.

076 Overall, our theoretical and empirical results highlight key modeling differences between GR and
 077 DR, showing that GR avoids DR’s bottlenecks and has greater potential as an IR paradigm at larger
 078 data and model scales. However, our experiments are limited to in-distribution queries, and neither
 079 the model nor the data scale is arbitrarily large. In practice, GR does not consistently outperform
 080 DR, as its effectiveness depends on factors such as docid design (Bevilacqua et al., 2022; Li et al.,
 081 2023b), training data construction (Zhuang et al., 2022), and decoding strategies (Zeng et al., 2024a;
 082 Lee et al., 2022). We conclude by discussing these limitations and outlining future directions to
 083 close the gap between GR’s theoretical promise and practical performance.

084 2 PRELIMINARIES

085 **Problem statement.** Let \mathcal{Q} be a set of queries and $\mathcal{D} = d_1, \dots, d_N$ a document collection. Let
 086 $P^*(d | q)$ denote the unknown ground-truth conditional distribution of documents given query q .
 087 Training pairs (q, d^+) are drawn from a data distribution $\mathcal{D}_{\text{train}}$, where d^+ is a relevant document
 088 under $P^*(\cdot | q)$. The goal of IR is to approximate $P^*(d | q)$ using a parametric model $P_\Theta(d | q)$,
 089 ensuring both probabilistic calibration and high ranking quality (Chowdhury, 2010).

090 **Dense retrieval.** Let $e_q \in \mathbb{R}^r$ and $e_d \in \mathbb{R}^r$ denote the query and document embeddings from
 091 encoders f_q and f_d , respectively (Karpukhin et al., 2020; Xiong et al., 2020a). The DR score for a
 092 pair is computed as their inner product $S(q, d) = e_q^\top e_d$, and the locally normalized (e.g., in-batch)
 093 softmax loss is defined accordingly:

$$094 P_\Theta(d | q; \mathcal{N}) = \frac{\exp(S(q, d) / \tau)}{\sum_{d' \in \{d\} \cup \mathcal{N}(q)} \exp(S(q, d') / \tau)}, \quad (1)$$

095 where $\mathcal{N}(q)$ is the negative set and $\tau > 0$ is a temperature. The standard contrastive objective is:

$$096 \mathcal{L}_{\text{DR}}(\Theta) = \mathbb{E}_q [-\log P_\Theta(d^+ | q; \mathcal{N}(q))]. \quad (2)$$

097 Eq. 2 encourages $S(q, d^+)$ to exceed the scores of negatives within the current candidate pool.
 098 In practice, negatives may come from the in-batch sampling (Karpukhin et al., 2020; Khattab &
 099 Zaharia, 2020) or hard-negative mining (Xiong et al., 2020a; Zhan et al., 2021).

100 **Generative retrieval.** Each document has a tokenized docid $y_{1:L} \in \mathcal{V}^L$ from a finite vocabulary \mathcal{V}
 101 (Tay et al., 2022). The GR training loss is defined by a sequence generation model $p_\Theta(y_t | y_{<t}, q)$:

$$102 \mathcal{L}_{\text{GR}}(\Theta) = \mathbb{E}_q [-\log P_\Theta(d^+ | q)] = \mathbb{E}_q \left[-\sum_{t=1}^L \log p_\Theta(y_t^+ | y_{<t}^+, q) \right]. \quad (3)$$

108 The mapping between sequences in \mathcal{V}^L and \mathcal{D} is constrained, so that decoding a sequence deterministically selects a document. At inference time, beam search is used with prefix constraints (e.g.,
 109 trie) to guarantee valid docids.
 110

112 **3 THEORETICAL ANALYSIS**

114 **3.1 LEARNING OBJECTIVES**

116 Here, we refer to an objective as *local* when normalization is restricted to the sampled candidate set,
 117 whereas a *global* objective normalizes over the entire document collection \mathcal{D} . §3.1.1 presents DR’s
 118 locally normalized surrogate and formalizes the resulting calibration gap, while §3.1.2 then shows
 119 that GR optimizes a globally normalized likelihood objective.
 120

121 **3.1.1 DR LOCALLY NORMALIZES SURROGATE**

123 The DR objective in Eq. 2 minimizes a surrogate defined on the set $\{d^+\} \cup \mathcal{N}(q)$, renormalizing
 124 scores via a softmax within K candidates per batch. This makes the learning objective explicitly
 125 dependent on the sampled negatives, implying that the negative-sampling scheme (both the size of
 126 the candidate set and the quality of the negatives) has a substantial impact on the final performance
 127 of DR. Ideally, one would use as negatives the entire set of non-relevant documents, but this is
 128 computationally infeasible under realistic resource constraints (Wang & Isola, 2020). This mismatch
 129 leads to a calibration gap between the global and local objectives.
 130

131 *Assumptions.* Negatives for each query q are drawn i.i.d. from a proposal sample policy $\pi(\cdot)$ over \mathcal{D}
 132 (with $\mu(\cdot)$ the random sample policy) and scores are bounded as $|S(q, d)/\tau| \leq M$. We define the
 133 proposal-bias term

$$\delta(q) = \log \mathbb{E}_{d \sim \pi} [e^{S(q, d)/\tau}] - \log \mathbb{E}_{d \sim \mu} [e^{S(q, d)/\tau}]. \quad (4)$$

134 **Theorem 3.1** (Lower bound under local normalization). *Let $\tilde{P}_\Theta(d | q)$ be the full-softmax distribution.
 135 Under the assumptions above, the expected gap satisfies the following condition:*

$$\mathbb{E}_q \left[\log \tilde{P}_\Theta(d^+ | q) - \log P_\Theta(d^+ | q; \mathcal{N}(q)) \right] \geq \log \frac{N}{K} - \mathbb{E}_q [\delta(q)], \quad (5)$$

136 where $N = |\mathcal{D}|$ and K is the batch candidate size.
 137

138 The proof in Appendix B exposes the mechanism: local normalization replaces the global partition
 139 function $Z(q)$ with a batch-level $Z_K(q)$ and, in expectation, $Z_K(q) \approx (K/N)Z(q)$ up to proposal
 140 bias, yielding a gap that shrinks only logarithmically in K , where $Z(q) = \sum_{d'} \exp(S(q, d')/\tau)$
 141 and $Z_K(q) = \sum_{d' \in \{d^+\} \cup \mathcal{N}(q)} \exp(S(q, d')/\tau)$. And a high-probability tail bound version of this
 142 theorem is provided in Appendix E.
 143

144 **Practical mitigations for the calibration gap.** Increasing K and mining harder negatives can
 145 partially reduce the gap by better approximating the global normalization, and temperature scaling or
 146 post-hoc calibration further helps align scores (Xiong et al., 2020a; Zhan et al., 2021). Nevertheless,
 147 as the corpus size N grows, the $\log(N/K)$ term dominates unless K scales proportionally with N ,
 148 making it increasingly hard for DR to match the true posterior calibration.
 149

150 **3.1.2 GR FULLY NORMALIZES MAXIMUM LIKELIHOOD**

151 The GR loss in Eq. 3 is the token-level negative log-likelihood of a fully normalized sequence model
 152 over docids. Averaging over tokens and queries, the cross-entropy decomposes as
 153

$$\underbrace{\mathbb{E}_q [-\log P_\Theta(d^+ | q)]}_{\text{CE loss}} = \underbrace{\mathbb{E}_q [H(P^*(\cdot | q))]}_{\text{entropy term}} + \underbrace{\mathbb{E}_q [\text{KL}(P^*(\cdot | q) \| P_\Theta(\cdot | q))]}_{\text{KL divergence}}. \quad (6)$$

154 From the CE–KL decomposition in Eq. 6, the entropy term is constant with respect to the model
 155 parameters Θ . We therefore obtain the following proposition, for which a detailed proof is provided
 156 in Appendix A:
 157

162 **Proposition 3.2** (Global normalization and calibration of GR). *Minimizing the GR loss in Eq. 3 is*
 163 *equivalent to minimizing the expected KL divergence in Eq. 6. Consequently, GR permits error-free*
 164 *approximation of the true posterior $P^*(d | q)$ and its objective is equivalent to likelihood-consistent*
 165 *optimization over the globally normalized candidate space.*

166 Note that teacher forcing makes gradients local to each conditional step, yet the objective itself
 167 remains globally normalized. Therefore, even under prefix constraints on the valid code space,
 168 improvements in likelihood translate directly into better probability calibration of $P_\Theta(d | q)$.
 169

170 **GR is expected to benefit under corpus scaling.** Based on the above analysis, we conclude that
 171 under the assumptions in §3.1.1 for locally normalized DR (fixed negative-sample budget K and
 172 proposal bias $\delta(q)$) the gap between the ideal global partition $Z(q)$ and its sampled counterpart
 173 $Z_K(q)$ grows with $\log N$ when K and δ are not increased along with the corpus growth. In practice,
 174 this typically manifests as saturation or degradation in retrieval metrics unless K is increased or the
 175 sample quality is improved. In contrast, GR optimizes a globally normalized likelihood over the
 176 docid space. Assuming a fixed docid scheme with adequate coverage and in-distribution queries,
 177 GR does not incur the $\log N$ calibration drift and can keep benefiting from larger corpora without
 178 increasing K (albeit with higher computational costs).
 179

180 3.2 REPRESENTATIONAL CAPACITY

181 §3.2.1 below shows that DR compresses relevance into rank- r structures, inducing a low-rank bot-
 182 tleneck on the relevance matrix, while §3.2.2 shows that GR can approximate the query-document
 183 posterior arbitrarily well using its full parameterization.

184 3.2.1 DR EXHIBITS A LOW-RANK BOTTLENECK IN RELEVANCE REPRESENTATION

185 DR learns a text-to-embedding mapping and computes relevance through a fixed post-interaction
 186 rule, typically a bilinear score such as the inner product $S(q, d) = e_q^\top e_d$. Consequently, all relevance
 187 information for a query or a document is compressed into an r -dimensional vector (Weller et al.,
 188 2025). Formally, DR stacks m query embeddings into $Q \in \mathbb{R}^{m \times r}$ and N document embeddings
 189 into $D \in \mathbb{R}^{N \times r}$. The resulting relevance matrix is $S = QD^\top \in \mathbb{R}^{m \times N}$, which satisfies
 190 $\text{rank}(S) \leq r$ regardless of the encoder architecture, as long as the final interaction is bilinear.
 191

192 By the Eckart-Young-Mirsky theorem (Eckart & Young, 1936; Mirsky, 1960), among all matrices
 193 of rank at most r , the truncated SVD of any target logit matrix S^* achieves the best Frobenius-
 194 norm approximation, with minimal error equal to the sum of squared discarded singular values. We
 195 therefore state the following corollary:

196 **Corollary 3.3** (Low-rank bottleneck of bilinear DR). *Let r be the embedding dimension. Any bi-*
 197 *linear DR with score $S(q, d) = e_q^\top e_d$ induces a relevance matrix $S = QD^\top$ with $\text{rank}(S) \leq r$.*
 198 *Moreover, for a target S^* , the optimal rank- r approximation error equals the squared singular-value*
 199 *tail $\sum_{i>r} \sigma_i(S^*)^2$.*
 200

201 Whenever S^* exhibits a heavy spectral tail, a fixed- r DR model inevitably suffers from an irreducible
 202 approximation error unless r is increased. Contemporaneous work (Weller et al., 2025) also identifies
 203 this limitation of DR, providing detailed proofs and experiments, and argues that late-interaction
 204 MVDR models (e.g., ColBERT (Khattab & Zaharia, 2020)) may mitigate the issue. However, we
 205 show that MVDR remains subject to a similar upper bound when tokens are grouped into channels
 206 (see Appendix D for details).

207 3.2.2 GR DIRECTLY FITS THE QUERY-DOCUMENT RELEVANCE MAPPING

208 Let \mathcal{V}^L denote the docid space with a fixed bijection to documents. GR directly fits the query-
 209 document relevance mapping through its full set of model parameters.

210 **Theorem 3.4** (Approximation of P^* by GR). *For any $\epsilon > 0$ and any conditional distribution*
 211 *$P^*(\cdot | q)$ supported on \mathcal{D} , there exist L and a decoder parameterization such that the induced GR*
 212 *model satisfies $\mathbb{E}_q[\text{TV}(P^*(\cdot | q), P_\Theta(\cdot | q))] < \epsilon$, where TV denotes the total variation distance.*
 213

214 Theorem 3.4 states that under a fixed bijective docid coding and for in-distribution queries, a suf-
 215 ficiently expressive GR model can approximate the true query-document relevance mapping arbi-

trarily well (in expected total-variation distance). In other words, with adequate capacity, GR could represents documents, queries, and their relevance relations within the model itself. Note that Theorem 3.4 continues to hold when GR decodes under prefix-constrained decoding (see Appendix C for a detailed proof). Nevertheless, in practice the degree to which GR fits the query-document mapping is affected by several factors, including the quality of the docid tree design and the sufficiency and cleanliness of training data (Tay et al., 2022; Zhuang et al., 2022; Wang et al., 2022). Therefore, Theorem 3.4 is a capacity statement rather than a claim about sample or compute efficiency. It assumes an in-distribution query law and a fixed docid. A highly unbalanced or semantically incoherent docid trie can increase optimization difficulty even under universality, and no guarantee is made for out-of-distribution queries.

GR is expected to benefit under model scaling. Under the representation analysis in §3.2, GR can reduce the posterior approximation error by scaling its model capacity (given a fixed docid scheme), whereas DR with bilinear interactions is constrained by an effective rank bound $\text{rank}(S) \leq r$ (or $\leq cr$ with c independent interaction channels). Hence, matching a heavy spectral tail requires proportionally increasing r or c . This predicts steeper gains for GR under equal-parameter scaling.

4 EXPERIMENTS

We present: (i) experiments that evaluate the theoretical limitations of DR, (ii) synchronized scaling experiments comparing GR and DR, and (iii) experiments that investigate the potential scaling advantages of GR.

4.1 EXPERIMENTAL SETUP

We evaluate on two widely used retrieval benchmarks: (i) *Natural Questions (NQ)* (Kwiatkowski et al., 2019): Real user questions paired with supporting evidence from Wikipedia; and (ii) *MS MARCO Passage* (Bajaj et al., 2016): Web search queries from Bing with associated relevant passages. We report the calibration metric *Brier*, computed as the mean squared error between the predicted relevance probability for the top-1 candidate and the ground truth for each query. We also report three retrieval metrics: (i) *Hits@k*, (ii) *NDCG@k*, and (iii) *MRR@k*.

We implement representative systems for DR and GR, deliberately avoiding sophisticated variants to ensure fairness and transparency. For DR, we use: (i) a *standard dual encoder* with inner-product scoring (referred to as *Standard DR*), following DPR (Karpukhin et al., 2020); and (ii) a *multi-vector late-interaction* variant (referred to as *MVDR*) in the style of COLBERT-v1 (Khattab & Zaharia, 2020). For GR, we adopt two docid designs and follow a DSI-style training/inference pipeline (Tay et al., 2022): (i) *codebook docids* constructed via residual quantization, where each docid is a length-6 sequence of 8-bit code indices (referred to as *GR-codebook*); and (ii) *text docids* that directly use the document title as the identifier (referred to as *GR-text*). All GR decoding is prefix-constrained by a trie built from the set of valid docids.

To control for capacity and pretraining, all DR models are built on Qwen3-Embedding-0.6B, and all GR models use Qwen3-0.6B (Yang et al., 2025a). **Full details of the experimental setup are provided in Appendix F, and the implementation details for each subsequent experiment are given in Appendix G.**

4.2 LIMITATIONS OF DR

Optimization limitations introduced by local normalization. To evaluate the effect of local normalization in DR, we fix all other settings and vary only the number of negative samples and the proportion of hard negatives, and then observe the resulting performance changes.

Figure 1 shows how DR performance changes as the number of negative samples increases. We observe that (i) the calibration metric Brier and the ranking metrics move in tandem, indicating that the theoretically predicted calibration drift manifests as changes in retrieval performance; (ii) all retrieval metrics improve as the number K of negative samples increases and have not plateaued within our compute budget; and (iii) despite a few outliers, Standard DR and MVDR exhibit broadly consistent trends across both datasets.

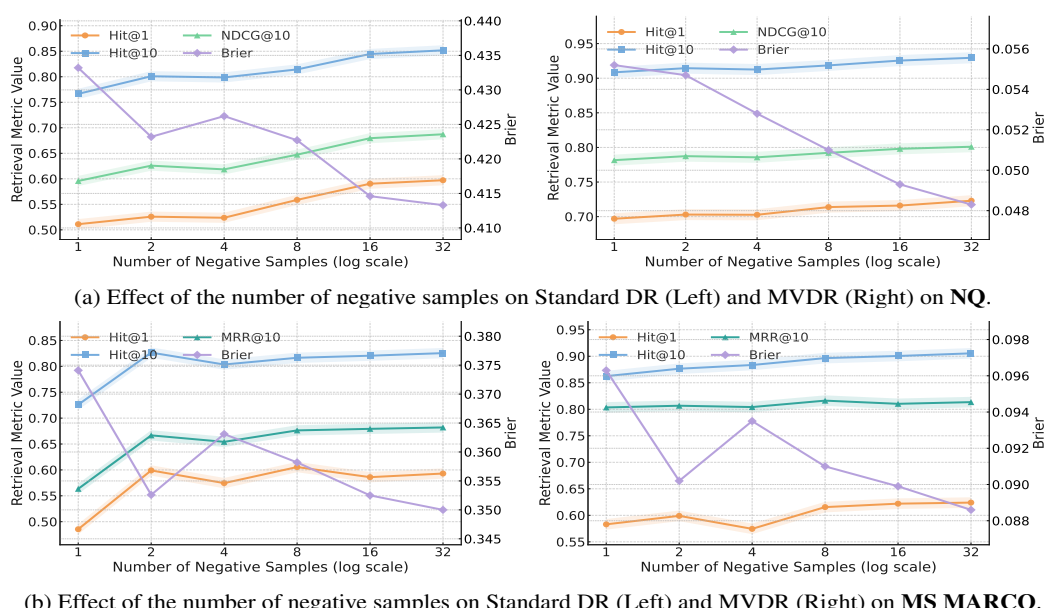


Figure 1: DR’s retrieval performance improves as the number of negative samples increases. The left y -axis shows retrieval metrics (higher is better), while the right y -axis shows the Brier score (lower is better). The plotted Brier values are raw and thus not comparable across different settings.

Table 1 shows the effect of the *negative-sampling strategy*, showing that DR is highly sensitive to how negatives are chosen. For example, when hard negatives constitute one half of the batch, Standard DR’s Hit@1 drops by about 13% relative to using no hard negatives, whereas MVDR’s Hit@1 actually improves when mixing in 1/4 hard negatives. These findings further corroborate the bias introduced by local normalization and indicate that mitigating this limitation purely via negative-sampling heuristics (e.g., injecting hard negatives) is nontrivial.

Table 1: Effect of the hard-negative ratio on DR and MVDR on the NQ dataset.

Hard-negative ratio	Standard DR				MVDR		
	Hit		NDCG		Hit		NDCG
	@1	@10	@10	@10	@1	@10	
0	52.4	79.9	61.9	57.5	80.4	61.9	
0.25	45.4	70.3	53.0	58.4	82.4	53.0	
0.5	39.5	63.2	46.7	52.2	78.8	46.7	
0.75	43.0	66.8	50.2	60.0	83.5	50.2	
1.0	47.0	73.8	52.2	55.6	81.6	50.2	

Representational limitations imposed by embedding dimensionality. To assess the limitations under bilinear interactions in DR, we vary the embedding size experimentally. Specifically, we append a two-layer non-linear projection after the original output layer to obtain the target embedding dimension, and train this projection jointly with the backbone.

The relationship between embedding dimensionality and DR performance is shown in Figure 2. We observe that: (i) the calibration metric and the ranking metrics vary consistently, indicating that the theoretical effect translates directly into retrieval outcomes; (ii) increasing the embedding dimension yields substantial improvements for both Standard DR and MVDR across datasets, with Standard DR achieving gains of over 20% on the NQ and MS MARCO datasets; and (iii) even at 1024 dimensions, well above the commonly used 768, retrieval performance continues to improve on nearly all curves. Since our datasets are much smaller than real-world corpora, these findings suggest that embedding dimensionality can act as a genuine bottleneck for dimensionality reduction.

4.3 SCALING TRENDS OF GR AND DR

GR and DR under corpus scaling. To assess how normalization schemes affect corpus-level scaling, we compare GR and DR on progressively larger corpora. We sample document and query subsets of varying sizes from the official training and evaluation sets, and train/evaluate GR and DR on matched subset sizes. All hyperparameters are held fixed except corpus size. To isolate training budget effects, we keep it fixed and vary only the number of candidate documents, increasing it logarithmically from a base equal to the number of documents seen during training (300K for NQ and 1M for MS MARCO).

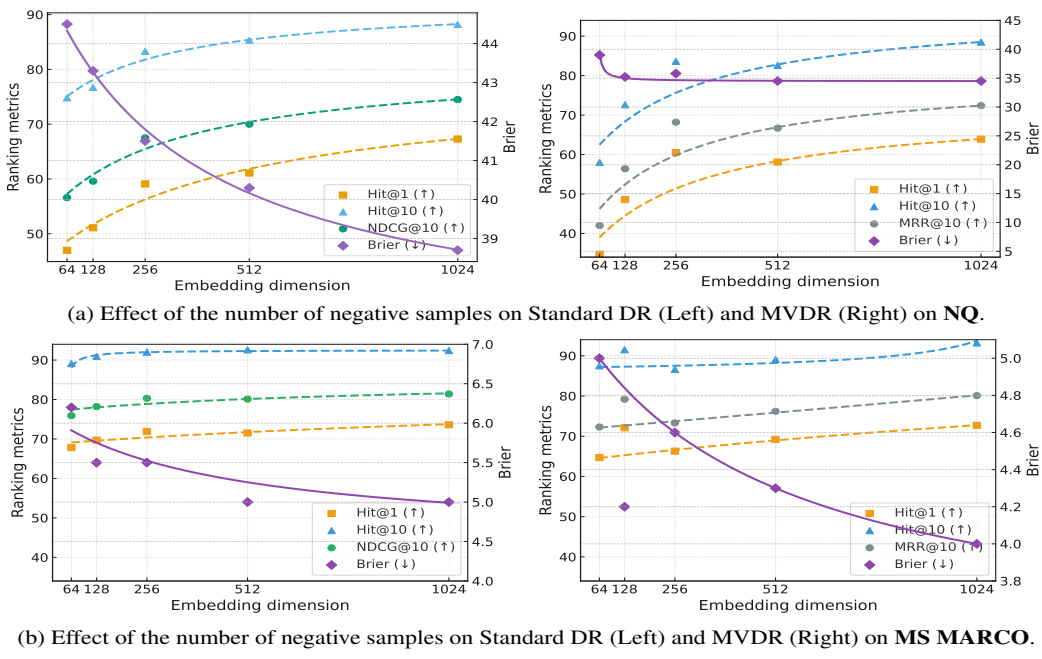


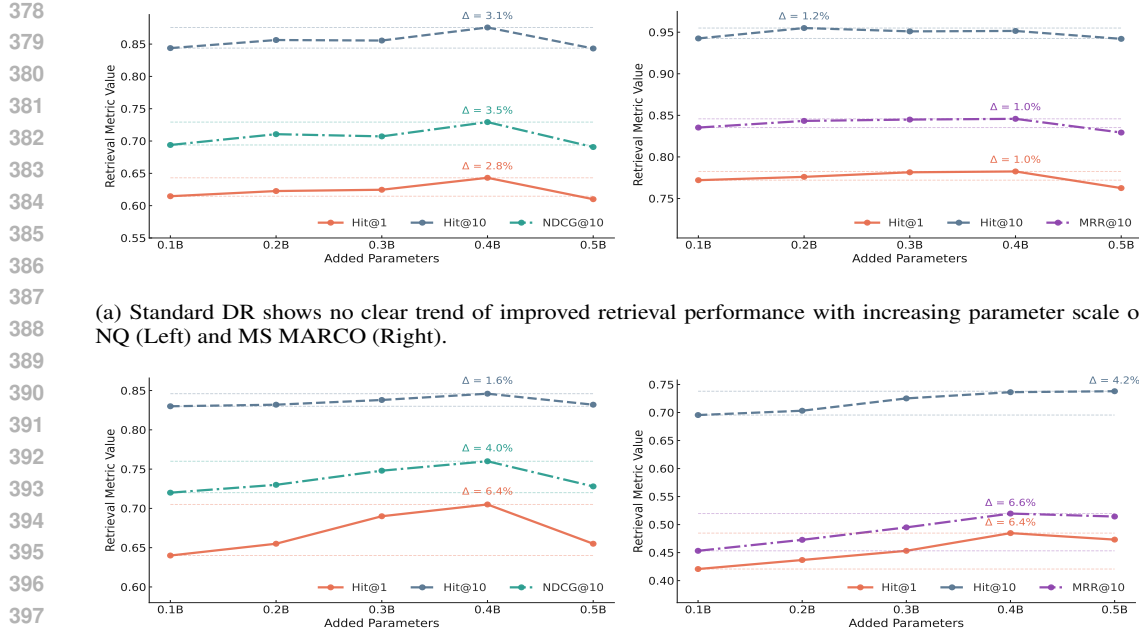
Figure 2: DR’s retrieval performance improves as the embedding dimension increases.

As shown in Table 2 (a) and Table 2 (b), both datasets exhibit the same pattern: (i) as the number of candidate documents increases, the performance of both GR and DR declines, reflecting the increased task difficulty introduced by a larger candidate pool; however, (ii) GR degrades more slowly than DR, both in magnitude and in rate. For instance, on NQ, DR’s Hit@1 decreases by 6.9% and Hit@10 by 6.3%, while GR’s Hit@1

and Hit@10 drop by only 3.3% each. This aligns with our theoretical analysis: corpus expansion amplifies the optimization drift of DR caused by local sampling, whereas GR optimizes a globally normalized objective over the full docid space for each query, making it less sensitive to additional non-relevant documents. Results for MVDR and GR-text are provided in Appendix H.

GR and DR under model scaling. To examine differences in model scaling, we compare GR and DR under equal added parameter budgets. We attach randomly initialized adapters of the same size to both models and train the adapters jointly with the backbone, then track ranking metrics. Note that the adapters range from 0.1B to 0.8B parameters and at the largest setting, the adapter exceeds the backbone in size, making this setup meaningful for model-scaling evaluation.

Figure 3 shows a clear upward trend for GR with the model scale. Performance improves substantially as parameters increase. On both datasets (NQ and MSMARCO), all metrics rise by roughly 5%, indicating that GR reaps sizable gains from added parameters. In contrast, DR remains flat or improves only marginally, with changes around 1%, suggesting that simply scaling parameters does not directly benefit DR. These patterns are consistent across both datasets. Taken together, the results imply that, in the era of large language models, GR is better positioned to capitalize on rapid parameter growth, whereas DR lacks an equally direct path and may require larger embeddings or richer contrastive pretraining. Please refer to Appendix I for results on MVDR and GR-text.



(a) Standard DR shows no clear trend of improved retrieval performance with increasing parameter scale on NQ (Left) and MS MARCO (Right).

(b) GR shows a clear upward scaling trend in retrieval performance on NQ (Left) and MS MARCO (Right).

Figure 3: Comparison of DR and GR under synchronized model scaling. Only the increasing range is shown here. All models drop after 0.4B due to adding too many new parameters. See Appendix I for the full curve.

4.4 POTENTIAL ADVANTAGES OF GR

Next, we explore GR’s advantages at larger scales using a 14B-parameter model. We focus on GR-text on the NQ dataset, as these experiments are designed to fully leverage capabilities acquired during LLM pretraining. The NQ dataset’s documents are drawn from Wikipedia, with titles serving as natural text docids. Because both documents and titles are seen during pretraining, this setup directly exploits the model’s world knowledge and reasoning abilities.

Zero-shot GR. GR performs token-by-token prediction of a docid and when the docid is textual, this inference procedure aligns with the LLM’s next-token-prediction (NTP) pretraining objective. This motivates the hypothesis that an LLM can perform retrieval without any task-specific training, relying solely on its pretrained capabilities. We therefore design a zero-shot GR experiment to test this hypothesis. Specifically, we add only a prompt and enforce decoding under trie constraints, with no retrieval-specific fine-tuning.

TTS GR. We further assess test-time scaling (TTS) with a “think-then-retrieve” procedure to probe GR’s exploitation of LLM capabilities and its internalization of the corpus. Specifically, before constrained decoding, the model first produces a short free-form reasoning snippet. The original query and the reasoning are then concatenated and passed to constrained decoding for retrieval. This augmentation is applied only at inference, while training follows the standard GR setup.

Results for zero-shot GR and TTS GR, alongside standard GR, are reported in Table 3. We summarize: (i) zero-shot GR achieves non-trivial retrieval quality (although it remains modest), suggesting that with larger models, carefully designed prompts, and suitable docids, practical training-free GR may be attainable; and (ii) even without task-specific fine-tuning, GR benefits from a pre-retrieval reasoning step, outperforming the no-reasoning baseline, which indicates that GR’s parameterized internalization of documents and relevance aids retrieval via query reformulation. These experiments corroborate GR’s advantages at larger model scales.

Table 3: Retrieval performance on the NQ dataset for standard GR-text and its zero-shot and TTS variants.

	Hit@1	Hit@10	NDCG@10
Zero-shot GR	18.1	23.8	33.3
Standard GR	45.7	63.5	88.6
TTS GR	47.3	65.8	89.1

432

5 DISCUSSION

433
 434
 435 **Practical challenges of GR.** Although GR is theoretically appealing and exhibits demonstrable
 436 scaling advantages, it seldom reaches the theoretical optimum in practice, for two main reasons:
 437 (i) Noisy or biased supervision (e.g., conflicting relevance labels) and insufficient training can induce
 438 an irreducible mismatch between the learned model and the target posterior (Zhuang et al., 2022);
 439 and (ii) Prefix-constrained autoregressive decoding is prone to error propagation which means once
 440 early tokens deviate, subsequent steps tend to drift (Bevilacqua et al., 2022; Zhang et al., 2024).
 441 This issue is exacerbated when the docid design is flawed (e.g., unbalanced hierarchies, suboptimal
 442 clustering, or text-based docids that fail to cover document content). Beyond this optimality gap,
 443 engineering considerations further limit GR’s practical use: (i) GR’s token-by-token decoding in-
 444 troduces high per-step latency whereas ANN-indexed DR can provide near-instant lookups once the
 445 index is built; and (ii) under continual corpus drift, GR often needs retraining or local fine-tuning to
 446 accommodate an updated codebook or shifting hierarchical boundaries (Chen et al., 2023; Kishore
 447 et al., 2023), whereas DR commonly supports index-only updates.

448 **Potential solutions.** We discuss some potential solutions to address the practical challenges of GR.
 449 For *data noise and undertraining*, two complementary directions are promising: (i) treating relevance
 450 itself as the pretraining target and pretrain a decoder-only model from scratch on large-scale,
 451 noise-controlled (q, d) pairs to directly optimize $-\log P(d | q)$, similar to some recent works on
 452 generative recommendation (e.g., one-rec (Deng et al., 2025)). This is appropriate when relevance is
 453 explicitly defined by human rules (e.g., e-commerce query–item (Rajput et al., 2023), ads matching
 454 (Fan et al., 2019), FAQ–KB pairs (Sakata et al., 2019)); and (ii) exploiting the world knowledge and
 455 reasoning of LLM bases. Specifically, teach the model the semantics and interface of retrieval with
 456 light instruction tuning instead of memorizing full-corpus relevance. At inference, execute “retrieval
 457 as constrained generation” via constrained decoding. This is suitable when the relevance underlying
 458 the retrieval task is already encoded in the pretraining corpus (e.g., Wikipedia or encyclopedic
 459 retrieval (Petroni et al., 2020)).

460 For *early-error propagation*, relaxing clustering constraints or decoding constraints might work.
 461 Specifically, allowing each document to belong to multiple clusters (especially for boundary cases)
 462 might reduce early-errors. On the decoding side, enabling backoff mechanisms or, when necessary,
 463 allowing tokens outside the constraint set to recover from early mistakes.

464 For *engineering efficiency*, integrating GR with DR in a single system within a single system is
 465 promising. One practical design is to let GR decode only a shallow prefix to perform coarse-grained
 466 category recall, followed by DR for fine-grained retrieval within that category. This coarse-to-fine
 467 design is expected to leverages GR’s capacity to fit relevance while mitigating error accumulation
 468 and reducing the latency associated with deep prefix-constrained decoding down to docids.

469

6 CONCLUSION AND LIMITATIONS

470 We have systematically compared DR and GR in terms of learning objectives and representational
 471 capacity. Theoretically, GR performs globally normalized maximum likelihood over the docid
 472 space, thereby avoiding the calibration gap introduced by DR’s locally normalized contrastive learning.
 473 Moreover, under fixed bilinear interactions, DR is constrained by a low-rank bottleneck deter-
 474 mined by the embedding dimension, whereas GR admits higher-rank approximations. Empirically,
 475 results on the NQ and MS MARCO datasets show that calibration and ranking metrics corroborate
 476 these theoretical differences. Under comparable corpus and parameter scaling, GR achieves
 477 larger gains and further demonstrates advantages in zero-shot and test-time scaling. In summary,
 478 GR shows promise in overcoming DR’s bottlenecks, though several practical challenges remain.

479 This work also has several limitations: (i) our theoretical analysis assumes idealized formulations
 480 of GR and DR and does not fully account for the effects of training data, docid design, or decod-
 481 ing/search strategies; (ii) due to resource constraints, we were unable to compare GR and DR at
 482 larger model and corpus scales; (iii) our comparisons did not include state-of-the-art variants of
 483 GR and DR; and (iv) although we propose several potential extensions for GR, we did not conduct
 484 preliminary experiments to validate their effectiveness.

486 7 REPRODUCIBILITY STATEMENT
487

488 We summarize the steps we have taken to ensure reproducibility and point to where the relevant
 489 details can be found. The theoretical assumptions are stated in Section §3 and Appendices A–E,
 490 where we provide complete proofs for the CE–KL decomposition, the DR local-normalization gap,
 491 the low-rank bottleneck, and the universality of GR. Readers can map each claim in Section §3
 492 to its corresponding appendix proof. Our experimental setup, including model choices, datasets,
 493 evaluation metrics, and training/inference details are specified in Section §4.1 and Appendix F. We
 494 enumerate all experimental factors that affect the results (the size/quality of negative samples, em-
 495 bedding dimensionality, and corpus/model scaling) and provide their implementations and settings
 496 in Appendix G. For large-model experiments (zero-shot GR and TTS GR), we report implementa-
 497 tion details in Appendix G including the exact instructions/prompts.

498
499 REFERENCES
500

501 Payal Bajaj, Daniel Campos, Nick Craswell, Li Deng, Jianfeng Gao, Xiaodong Liu, Rangan Ma-
 502 jumder, Andrew McNamara, Bhaskar Mitra, Tri Nguyen, et al. Ms marco: A human generated
 503 machine reading comprehension dataset. *arXiv preprint arXiv:1611.09268*, 2016.

504 Michele Bevilacqua, Giuseppe Ottaviano, Patrick Lewis, Scott Yih, Sebastian Riedel, and Fabio
 505 Petroni. Autoregressive search engines: Generating substrings as document identifiers. *Advances*
 506 *in Neural Information Processing Systems*, 35:31668–31683, 2022.

507 Jiangui Chen, Ruqing Zhang, Jiafeng Guo, Maarten de Rijke, Wei Chen, Yixing Fan, and Xueqi
 508 Cheng. Continual learning for generative retrieval over dynamic corpora. In *Proceedings of the*
 509 *32nd ACM international conference on information and knowledge management*, pp. 306–315,
 510 2023.

511 Gobinda G Chowdhury. *Introduction to modern information retrieval*. Facet publishing, 2010.

512 Jiaxin Deng, Shiyao Wang, Kuo Cai, Lejian Ren, Qigen Hu, Weifeng Ding, Qiang Luo, and Guorui
 513 Zhou. Onerec: Unifying retrieve and rank with generative recommender and iterative preference
 514 alignment. *arXiv preprint arXiv:2502.18965*, 2025.

515 Carl Eckart and Gale Young. The approximation of one matrix by another of lower rank. *Psychome-
 516 trika*, 1(3):211–218, 1936.

517 Miao Fan, Jiacheng Guo, Shuai Zhu, Shuo Miao, Mingming Sun, and Ping Li. Mobius: towards
 518 the next generation of query-ad matching in baidu’s sponsored search. In *Proceedings of the 25th*
 519 *ACM SIGKDD International Conference on Knowledge Discovery & Data Mining*, pp. 2509–
 520 2517, 2019.

521 Yixing Fan, Xiaohui Xie, Yinqiong Cai, Jia Chen, Xinyu Ma, Xiangsheng Li, Ruqing Zhang, Jiafeng
 522 Guo, et al. Pre-training methods in information retrieval. *Foundations and Trends® in Information*
 523 *Retrieval*, 16(3):178–317, 2022.

524 Thibault Formal, Benjamin Piwowarski, and Stéphane Clinchant. Splade: Sparse lexical and ex-
 525 pansion model for first stage ranking. In *Proceedings of the 44th International ACM SIGIR*
 526 *Conference on Research and Development in Information Retrieval*, pp. 2288–2292, 2021.

527 Vladimir Karpukhin, Barlas Ouz, Sewon Min, Patrick SH Lewis, Ledell Wu, Sergey Edunov, Danqi
 528 Chen, and Wen-tau Yih. Dense passage retrieval for open-domain question answering. In *EMNLP*
 529 *(1)*, pp. 6769–6781, 2020.

530 Omar Khattab and Matei Zaharia. Colbert: Efficient and effective passage search via contextualized
 531 late interaction over bert. In *Proceedings of the 43rd International ACM SIGIR conference on*
 532 *research and development in Information Retrieval*, pp. 39–48, 2020.

533 Diederik P Kingma and Jimmy Ba. Adam: A method for stochastic optimization. *arXiv preprint*
 534 *arXiv:1412.6980*, 2014.

540 Varsha Kishore, Chao Wan, Justin Lovelace, Yoav Artzi, and Kilian Q Weinberger. Incdsi: In-
 541 crementally updatable document retrieval. In *International conference on machine learning*, pp.
 542 17122–17134. PMLR, 2023.

543 Tom Kwiatkowski, Jennimaria Palomaki, Olivia Redfield, Michael Collins, Ankur Parikh, Chris
 544 Alberti, Danielle Epstein, Illia Polosukhin, Jacob Devlin, Kenton Lee, et al. Natural questions: a
 545 benchmark for question answering research. *Transactions of the Association for Computational
 546 Linguistics*, 7:453–466, 2019.

547 Hyunji Lee, Jaeyoung Kim, Hoyeon Chang, Hanseok Oh, Sohee Yang, Vlad Karpukhin, Yi Lu, and
 548 Minjoon Seo. Nonparametric decoding for generative retrieval. *arXiv preprint arXiv:2210.02068*,
 549 2022.

550 JDMCK Lee and K Toutanova. Pre-training of deep bidirectional transformers for language under-
 551 standing. *arXiv preprint arXiv:1810.04805*, 3(8):4171–4186, 2018.

552 Mike Lewis, Yinhan Liu, Naman Goyal, Marjan Ghazvininejad, Abdelrahman Mohamed, Omer
 553 Levy, Veselin Stoyanov, and Luke Zettlemoyer. Bart: Denoising sequence-to-sequence pre-
 554 training for natural language generation, translation, and comprehension. In *Proceedings of the
 555 58th Annual Meeting of the Association for Computational Linguistics*, pp. 7871–7880, 2020.

556 Minghan Li, Sheng-Chieh Lin, Xueguang Ma, and Jimmy Lin. Slim: Sparsified late interaction for
 557 multi-vector retrieval with inverted indexes. In *Proceedings of the 46th International ACM SIGIR
 558 Conference on Research and Development in Information Retrieval*, pp. 1954–1959, 2023a.

559 Yongqi Li, Nan Yang, Liang Wang, Furu Wei, and Wenjie Li. Multiview identifiers enhanced gen-
 560 erative retrieval. *arXiv preprint arXiv:2305.16675*, 2023b.

561 Yongqi Li, Nan Yang, Liang Wang, Furu Wei, and Wenjie Li. Learning to rank in generative retrieval.
 562 In *Proceedings of the AAAI Conference on Artificial Intelligence*, volume 38, pp. 8716–8723,
 563 2024.

564 Leon Mirsky. Symmetric gauge functions and unitarily invariant norms. *The quarterly journal of
 565 mathematics*, 11(1):50–59, 1960.

566 Bhaskar Mitra, Nick Craswell, et al. An introduction to neural information retrieval. *Foundations
 567 and Trends® in Information Retrieval*, 13(1):1–126, 2018.

568 Thong Nguyen and Andrew Yates. Generative retrieval as dense retrieval. *arXiv preprint
 569 arXiv:2306.11397*, 2023.

570 Fabio Petroni, Aleksandra Piktus, Angela Fan, Patrick Lewis, Majid Yazdani, Nicola De Cao, James
 571 Thorne, Yacine Jernite, Vladimir Karpukhin, Jean Maillard, et al. Kilt: a benchmark for knowl-
 572 edge intensive language tasks. *arXiv preprint arXiv:2009.02252*, 2020.

573 Alec Radford, Karthik Narasimhan, Tim Salimans, Ilya Sutskever, et al. Improving language under-
 574 standing by generative pre-training. 2018.

575 Shashank Rajput, Nikhil Mehta, Anima Singh, Raghunandan Hulikal Keshavan, Trung Vu, Lukasz
 576 Heldt, Lichan Hong, Yi Tay, Vinh Tran, Jonah Samost, et al. Recommender systems with gener-
 577 ative retrieval. *Advances in Neural Information Processing Systems*, 36:10299–10315, 2023.

578 Wataru Sakata, Tomohide Shibata, Ribeka Tanaka, and Sadao Kurohashi. Faq retrieval using query-
 579 question similarity and bert-based query-answer relevance. In *Proceedings of the 42nd interna-
 580 tional ACM SIGIR conference on research and development in information retrieval*, pp. 1113–
 581 1116, 2019.

582 Yi Tay, Vinh Tran, Mostafa Dehghani, Jianmo Ni, Dara Bahri, Harsh Mehta, Zhen Qin, Kai Hui,
 583 Zhe Zhao, Jai Gupta, et al. Transformer memory as a differentiable search index. *Advances in
 584 Neural Information Processing Systems*, 35:21831–21843, 2022.

585 Ashish Vaswani, Noam Shazeer, Niki Parmar, Jakob Uszkoreit, Llion Jones, Aidan N Gomez,
 586 Łukasz Kaiser, and Illia Polosukhin. Attention is all you need. *Advances in neural informa-
 587 tion processing systems*, 30, 2017.

594 Tongzhou Wang and Phillip Isola. Understanding contrastive representation learning through align-
 595 ment and uniformity on the hypersphere. In *International conference on machine learning*, pp.
 596 9929–9939. PMLR, 2020.

597

598 Yujing Wang, Yingyan Hou, Haonan Wang, Ziming Miao, Shibin Wu, Qi Chen, Yuqing Xia, Cheng-
 599 min Chi, Guoshuai Zhao, Zheng Liu, et al. A neural corpus indexer for document retrieval. *Ad-*
 600 *vances in Neural Information Processing Systems*, 35:25600–25614, 2022.

601 Orion Weller, Michael Boratko, Iftekhar Naim, and Jinhyuk Lee. On the theoretical limitations of
 602 embedding-based retrieval. *arXiv preprint arXiv:2508.21038*, 2025.

603

604 Shiguang Wu, Wenda Wei, Mengqi Zhang, Zhumin Chen, Jun Ma, Zhaochun Ren, Maarten de Rijke,
 605 and Pengjie Ren. Generative retrieval as multi-vector dense retrieval. In *Proceedings of the 47th*
 606 *International ACM SIGIR Conference on Research and Development in Information Retrieval*,
 607 pp. 1828–1838, 2024.

608 Lee Xiong, Chenyan Xiong, Ye Li, Kwok-Fung Tang, Jialin Liu, Paul Bennett, Junaid Ahmed,
 609 and Arnold Overwijk. Approximate nearest neighbor negative contrastive learning for dense text
 610 retrieval. *arXiv preprint arXiv:2007.00808*, 2020a.

611 Lee Xiong, Chenyan Xiong, Ye Li, Kwok-Fung Tang, Jialin Liu, Paul Bennett, Junaid Ahmed,
 612 and Arnold Overwijk. Approximate nearest neighbor negative contrastive learning for dense text
 613 retrieval. volume abs/2007.00808, 2020b. URL <https://api.semanticscholar.org/CorpusID:220302524>.

614

615 An Yang, Anfeng Li, Baosong Yang, Beichen Zhang, Binyuan Hui, Bo Zheng, Bowen Yu,
 616 Chang Gao, Chengen Huang, Chenxu Lv, et al. Qwen3 technical report. *arXiv preprint*
 617 *arXiv:2505.09388*, 2025a.

618

619 An Yang, Bowen Yu, Chengyuan Li, Dayiheng Liu, Fei Huang, Haoyan Huang, Jiandong Jiang,
 620 Jianhong Tu, Jianwei Zhang, Jingren Zhou, et al. Qwen2. 5-1m technical report. *arXiv preprint*
 621 *arXiv:2501.15383*, 2025b.

622

623 Hansi Zeng, Chen Luo, Bowen Jin, Sheikh Muhammad Sarwar, Tianxin Wei, and Hamed Zamani.
 624 Scalable and effective generative information retrieval. In *Proceedings of the ACM Web Confer-*
 625 *ence 2024*, pp. 1441–1452, 2024a.

626

627 Hansi Zeng, Chen Luo, and Hamed Zamani. Planning ahead in generative retrieval: Guiding au-
 628 toregressive generation through simultaneous decoding. In *Proceedings of the 47th International*
 629 *ACM SIGIR Conference on Research and Development in Information Retrieval*, pp. 469–480,
 2024b.

630

631 Jingtao Zhan, Jiaxin Mao, Yiqun Liu, Jiafeng Guo, Min Zhang, and Shaoping Ma. Optimizing dense
 632 retrieval model training with hard negatives. In *Proceedings of the 44th international ACM SIGIR*
 633 *conference on research and development in information retrieval*, pp. 1503–1512, 2021.

634

635 Peitian Zhang, Zheng Liu, Yujia Zhou, Zhicheng Dou, Fangchao Liu, and Zhao Cao. Generative
 636 retrieval via term set generation. In *Proceedings of the 47th International ACM SIGIR Conference*
 637 *on Research and Development in Information Retrieval*, pp. 458–468, 2024.

638

639 Shengyao Zhuang, Houxing Ren, Linjun Shou, Jian Pei, Ming Gong, Guido Zuccon, and Dixin
 640 Jiang. Bridging the gap between indexing and retrieval for differentiable search index with query
 641 generation. *arXiv preprint arXiv:2206.10128*, 2022.

642

643

644

645

646

647

648 A CROSS-ENTROPY AND KL DECOMPOSITION

650 For completeness, we give a concise derivation of Eq. 6. Let P be the data distribution and Q_Θ the
 651 model on the same finite support. By definition,

$$653 \text{CE}(P, Q_\Theta) = \mathbb{E}_{x \sim P}[-\log Q_\Theta(x)] = \mathbb{E}_{x \sim P}\left[\log \frac{P(x)}{Q_\Theta(x)}\right] + \mathbb{E}_{x \sim P}[-\log P(x)]. \quad (7)$$

655 The first term equals $\text{KL}(P\|Q_\Theta)$ and the second equals $H(P)$, hence $\text{CE}(P, Q_\Theta) = H(P) +$
 656 $\text{KL}(P\|Q_\Theta)$. For conditional sequence models (GR), summing token-wise cross-entropies yields
 657 the same identity after taking expectations over queries.

658 B PROOF OF THEOREM 3.1

661 For a query q , define the global and in-batch partition functions

$$662 Z(q) = \sum_{d' \in \mathcal{D}} \exp(S(q, d')/\tau), \quad Z_K(q) = \sum_{d' \in \{d^+\} \cup \mathcal{N}(q)} \exp(S(q, d')/\tau). \quad (8)$$

664 Then

$$665 \log \tilde{P}_\Theta(d^+ | q) - \log P_\Theta(d^+ | q; \mathcal{N}) = \log Z_K(q) - \log Z(q). \quad (9)$$

666 Let μ be the corpus marginal (uniform over \mathcal{D}) and π the negative-sampling proposal,

$$668 \delta(q) = \log \mathbb{E}_{d \sim \pi}[\text{e}^{S(q, d)/\tau}] - \log \mathbb{E}_{d \sim \mu}[\text{e}^{S(q, d)/\tau}]. \quad (10)$$

669 Taking expectation over the sampling of $\mathcal{N}(q)$ and using Jensen's inequality,

$$671 \mathbb{E}[\log Z_K(q)] \geq \log \mathbb{E}[Z_K(q)] \geq \log K + \log \mathbb{E}_{d \sim \pi}[\text{e}^{S(q, d)/\tau}], \quad (11)$$

672 where we use the fact that $\mathbb{E}[Z_K(q)] \geq K \mathbb{E}_{d \sim \pi}[\text{e}^{S(q, d)/\tau}]$. Since $Z(q) = N \mathbb{E}_{d \sim \mu}[\text{e}^{S(q, d)/\tau}]$, we
 673 obtain

$$674 \mathbb{E}[\log Z_K(q) - \log Z(q)] \geq \log \frac{K}{N} - \delta(q). \quad (12)$$

675 Averaging over queries gives Theorem 3.1.

678 C CONSTRUCTIVE UNIVERSALITY FOR GR

680 Fix a bijection between \mathcal{D} and the leaves of a $|\mathcal{V}|$ -ary trie of depth L . Given a target posterior
 681 $P^*(\cdot | q)$, assign at each internal node the conditional distribution over its children to match the
 682 subtree mass under P^* : for node u with children $\{v\}$, set

$$683 p^*(v | u, q) = \frac{\sum_{\text{leaves } \ell \in \text{subtree}(v)} P^*(\ell | q)}{\sum_{\text{leaves } \ell \in \text{subtree}(u)} P^*(\ell | q)}. \quad (13)$$

686 A decoder with sufficient capacity can approximate each local conditional $p^*(\cdot | u, q)$ arbitrarily
 687 well. By the chain rule along any root-to-leaf path, the product of these conditionals approximates
 688 the target leaf mass, hence the induced leaf distribution approaches $P^*(\cdot | q)$ in total variation.
 689 Under prefix-constrained decoding, the same construction applies because valid leaves are exactly
 690 the trie leaves corresponding to \mathcal{D} .

692 D LOW-RANK LIMITATION FOR DR

693 Let $S^* \in \mathbb{R}^{m \times N}$ be a ground-truth logit matrix whose (i, j) -entry is a monotone transform of
 694 $\log P^*(d_j | q_i)$. Any bilinear DR model with embedding dimension r factorizes as $S = QD^\top$ and
 695 thus $\text{rank}(S) \leq r$ (or $\leq cr$ with c independent interaction channels). By the Eckart-Young-Mirsky
 696 theorem,

$$697 \min_{\text{rank}(S) \leq r} \|S - S^*\|_F^2 = \sum_{i > r} \sigma_i(S^*)^2, \quad (14)$$

699 the squared Frobenius norm of the spectral tail beyond rank r .

701 Consequently, if S^* has a heavy spectral tail, any fixed- r DR model incurs an irreducible posterior
 702 approximation error unless r (or the number of interaction channels) is increased.

702 E A HIGH-PROBABILITY BOUND FOR $\log Z_K - \log Z$

704 Fix a query q and define $X = e^{S(q,d)/\tau}$ for $d \sim \pi(\cdot | q)$ with mean $\mu_\pi = \mathbb{E}_\pi[X]$ and variance
 705 $\sigma_\pi^2 = \text{Var}_\pi[X]$. Let X_1, \dots, X_K be i.i.d. copies and $\bar{X}_K = \frac{1}{K} \sum_{i=1}^K X_i$. Assuming X is sub-
 706 exponential (e.g., bounded or with a finite moment generating function in a neighborhood of 0), a
 707 Bernstein-type inequality gives, for any $\epsilon \in (0, 1)$,

$$709 \Pr \left[\log \bar{X}_K \leq \log \mu_\pi - \epsilon \right] \leq \exp \left(- \frac{K \epsilon^2}{2(\sigma_\pi^2/\mu_\pi^2 + \epsilon/3)} \right). \quad (15)$$

711 Since $Z_K(q) = \sum_{d \in \mathcal{N}(q)} e^{S(q,d)/\tau} = K \bar{X}_K$ and $Z(q) = N \mu_\mu$ with $\mu_\mu = \mathbb{E}_{d \sim \mu}[e^{S(q,d)/\tau}]$, we
 712 have with probability at least $1 - \exp(-cK\epsilon^2)$ (for a constant c depending on moments of X):

$$714 \log Z_K(q) - \log Z(q) \geq \log \frac{K}{N} - (\log \mu_\mu - \log \mu_\pi) - \epsilon = \log \frac{K}{N} - \delta(q) - \epsilon. \quad (16)$$

715 Averaging over q yields a high-probability version of Theorem 3.1. We emphasize that this bound
 716 holds under i.i.d. negatives from π ; for adaptive or “hard-negative” proposals $\pi_t(\cdot | q, \Theta_t)$, the same
 717 form holds with an additional bias term in $\delta_t(q)$ that captures proposal/model dependence.

719 F DETAILED EXPERIMENTAL SETUP

721 **Datasets.** We evaluate on two standard retrieval benchmark datasets: (i) **Natural Questions (NQ)**
 722 (Kwiatkowski et al., 2019). This is a collection of real-user questions paired with supporting
 723 Wikipedia evidence. We use the official train (313K) and test (7K) splits. To make generative
 724 retrieval feasible, we ensure that each test query’s gold document appears in the docid inventory con-
 725 structed from the training corpus (i.e., the gold docid is seen during training); and (ii) **MS MARCO**
 726 **Passage** (Bajaj et al., 2016). This is a set of web search queries from Bing with associated passages.
 727 We use the passage-ranking subset and sample 1M training pairs and 2K evaluation queries from
 728 the official train/test splits. Unlike NQ, we do not enforce the “seen-document” constraint on MS
 729 MARCO (because enforcing it would shrink the evaluation set to only few hundred queries).

730 **Models used for comparison.** We implement two representative systems for both DR and GR
 731 and intentionally avoid complex variants to keep comparisons fair and transparent. For DR, we
 732 implement (i) a *standard bi-encoder* in the spirit of DPR (Karpukhin et al., 2020) with inner-product
 733 scoring; and (ii) a *multi-vector late-interaction* variant like ColBERT v1 (Khattab & Zaharia, 2020).
 734 For GR, we implement two varying about the docid design and train/inference follow the DSI-style
 735 (Tay et al., 2022): (i) *codebook docids* built via residual quantization, each docid is a length-6
 736 sequence of 8-bit code indices; and (ii) *textual docids* that directly use the title as the document
 737 identifier. All GR decoding is prefix-constrained by a trie constructed from the set of valid docids.

738 **Metrics.** We report the calibration metric *Brier*, which is the mean squared error between the pre-
 739 dicted relevance probability and the ground truth over the query’s rank-1 candidate. We report
 740 unnormalized (raw) Brier scores, consequently, they are comparable only within the same dataset
 741 and experimental series, and the values are not comparable across experiments. We also report four
 742 retrieval metrics: (i) *Hits@k* indicates whether at least one relevant document appears in the top- k
 743 results for a query; (ii) *NDCG@k* is the normalized discounted cumulative gain at cutoff k , using
 744 binary gains with logarithmic discounting by rank; and (iii) *MRR@k* is the mean reciprocal rank of
 745 the first relevant document within the top- k .

746 **Training and inference.** To control for capacity and pretraining, all DR models are built on Qwen3-
 747 Embedding-0.6B, and all GR models use Qwen3-0.6B (Yang et al., 2025a). Unless otherwise noted,
 748 we train with the Adam optimizer (Kingma & Ba, 2014) using its default settings. At inference
 749 time, DR retrieves top- k candidates using FAISS-based ANN search (Xiong et al., 2020b), while
 750 GR performs top- k constrained decoding over the docid trie.

751 G DETAILED EXPERIMENTAL IMPLEMENTATION

754 **DR negative sampling.** The goal is to assess how negative sampling affects DR performance along
 755 two dimensions: size and quality. For size, we use random negatives and vary the number of neg-
 756 atives during training. For quality, we experiment only on NQ, which provides both standard and

756 hard negatives: we vary the proportion of hard negatives in the sampled batch. If the official hard
 757 negatives are insufficient, we first fill with the provided standard negatives, and if still insufficient we
 758 complete the batch with random negatives. In this experiment, both query and document embedding
 759 dimensionality is fixed at 128, and MVDR and DR share identical settings.

760 **DR embedding size.** The goal is to examine the constraint imposed by the embedding dimension on
 761 DR. We append a two-layer non-linear projection (ReLU activations) after the model’s output layer
 762 to map embeddings to the target dimension and this projection is trained jointly with the backbone.
 763 Random negative sampling is used, and MVDR shares the same settings as DR.

764 **Corpus scaling.** The goal is to observe how GR and DR behave when the training corpus size is
 765 increased by the same amount. We control the number of documents in the corpus and require that
 766 each document appears at least once as a positive in the training set; the test set is a subset of this
 767 corpus. In this experiment, DR uses random negative sampling and 128-dimensional embeddings.
 768 GR-codebook and GR-text follow the configurations described in the main text. GR-text is evaluated
 769 only on NQ, where the official titles can serve as textual docids.

770 **Model scaling.** The goal is to compare GR and DR when model capacity is scaled by the same
 771 budget. We equip each layer with randomly initialized adapters of matched size and control the
 772 scaling by the total number of newly introduced parameters and adapters are trained jointly with the
 773 backbone. Note that the largest adapter budget can exceed the original backbone size. All other
 774 settings mirror those in the Corpus Scaling experiment.

775 **GR zero-shot.** The goal is to evaluate GR’s retrieval ability without fine-tuning, relying solely
 776 on pretrained knowledge. This experiment is conducted only on NQ with the GR-text, because
 777 NQ’s documents and their titles (used as docids) come from Wikipedia which is thoroughly cov-
 778 ered during LLM pretraining making zero-shot GR feasible. We employ a larger model (Qwen3-
 779 14B) for this study. Specifically, we do not fine-tune Qwen3-14B, instead, we prepend a prompt
 780 to each query: Given the question, predict the document title that most
 781 likely contains the answer. The title is: and then enforce trie-constrained
 782 decoding to produce the docid.

783 **GR TTS.** The goal is to assess whether GR can leverage an LLM’s reasoning capabili-
 784 ty and its internalized document knowledge to improve performance via a “think-then-
 785 retrieve” procedure. This experiment is conducted only on NQ with the GR-text, us-
 786 ing Qwen3-14B as the backbone. During training, We prepend a retrieval instruction
 787 I_r to each query: Given the question, predict the document title that
 788 most likely contains the answer. The title is: and fine-tune GR with
 789 LoRA. During inference, the model first performs unconstrained “thinking” given the
 790 prompt: Briefly think about the document title that may contain the
 791 answer to this question. The generated reasoning is then concatenated with the origi-
 792 nal query and the retrieval instruction I_r , and constrained decoding is applied to produce the docid.

793
 794
 795
 796
 797
 798
 799
 800
 801
 802
 803
 804
 805
 806
 807
 808
 809

810 H EXTENDED RESULTS OF CORPUS SCALING

812 This section supplements the corpus scaling experiments in Section 4.3. Figure 4 presents the full
 813 performance trends under corpus scaling for all models (including MVDR and GR-text, which are
 814 not covered in the main text Table 2). The conclusions mirror those in the main text: overall, DR
 815 exhibits a larger performance drop than GR as the corpus size increases.

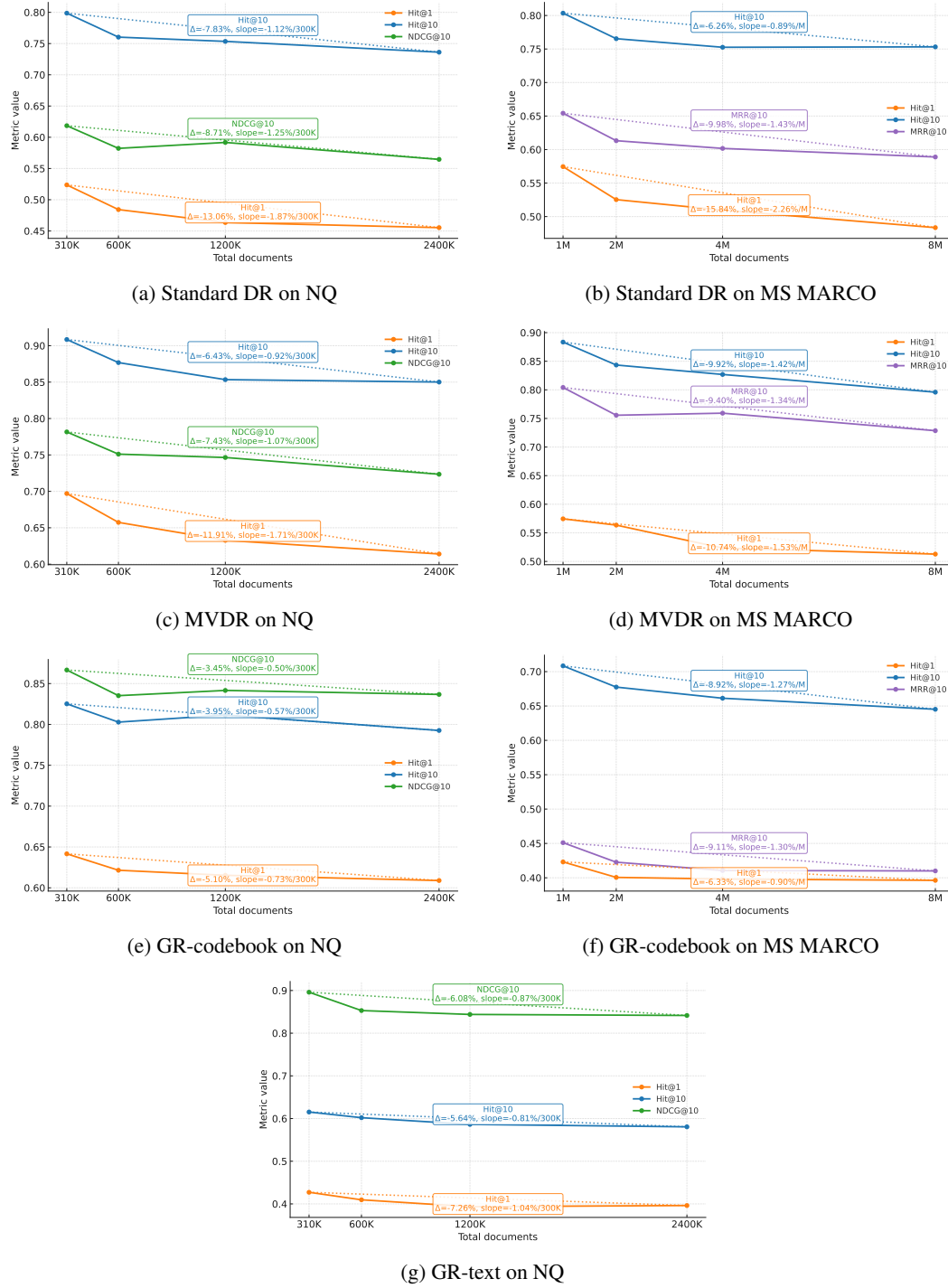
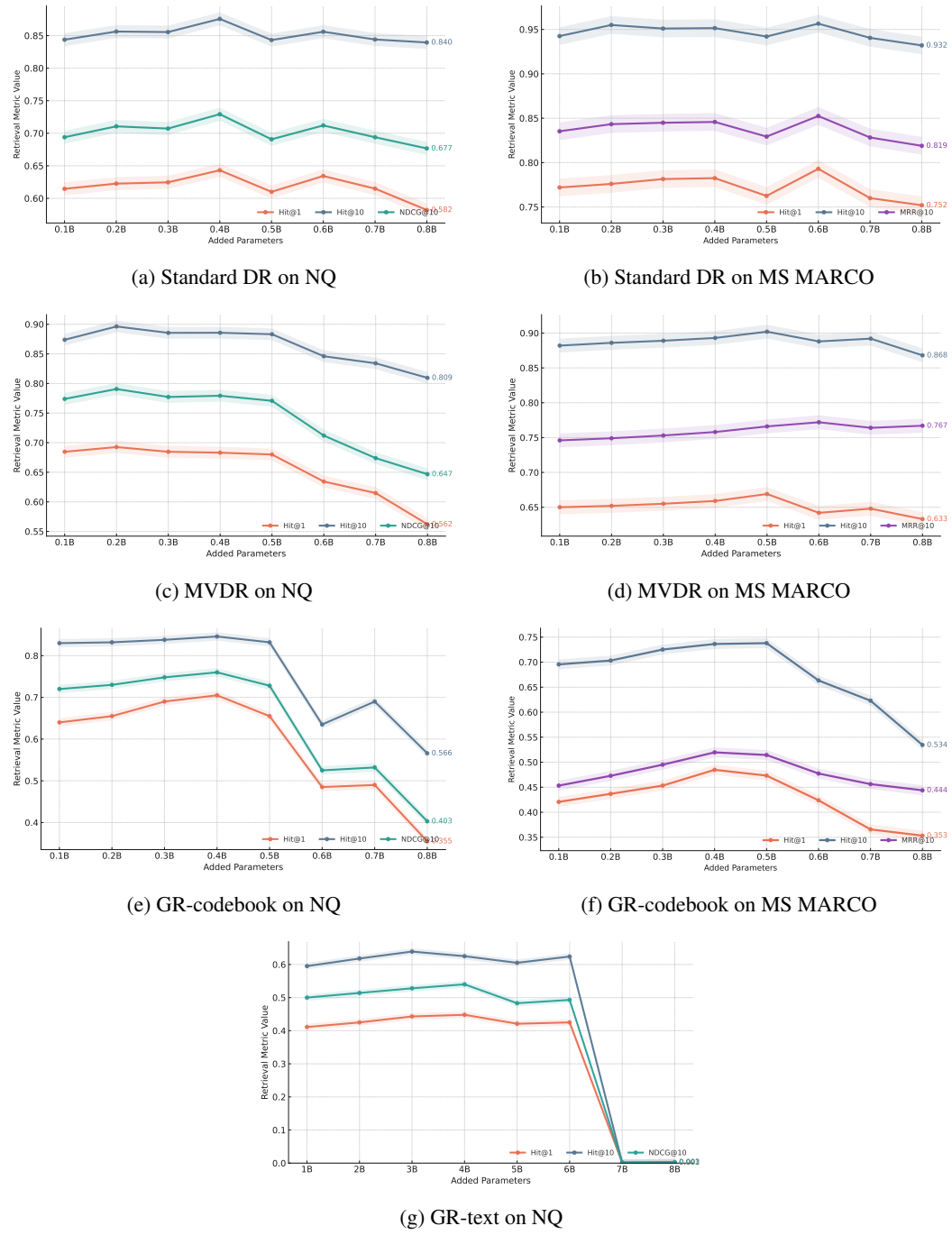


Figure 4: Extended results of corpus scaling.

864 I EXTENDED RESULTS ON MODEL SCALING
865

866 This section supplements the model scaling experiments in Section 4.3. Figure 5 presents the full
867 performance trends under model scaling for all models (including MVDR and GR-text, which are
868 not covered in the main text, Figure 3). The end-of-curve downturn observed in all traces is likely
869 due to the addition of excessive parameters. Ignoring this effect and focusing on the initial stage
870 where model scaling yields gains, the conclusion aligns with the main text: GR derives greater
871 benefits from increases in parameter scale.

915 Figure 5: Extended results of model scaling.
916
917

918 **J LLM USAGE**
919920 We used a large language model to help polish wording and to generate codes for data visualization.
921 All core ideas, theoretical analysis, experimental design, and the initial full manuscript were con-
922 ceived and written by all co-authors. All LLM-suggested text and code were reviewed and verified
923 by the authors before inclusion.924
925
926
927
928
929
930
931
932
933
934
935
936
937
938
939
940
941
942
943
944
945
946
947
948
949
950
951
952
953
954
955
956
957
958
959
960
961
962
963
964
965
966
967
968
969
970
971